

Measurement of the Depolarization of Reflected Light from Spectralon

D.A. Haner and B.T. McGuckin

**Jet Propulsion Laboratory
California Institute of Technology
4800 Oak Grove Drive
Pasadena CA 91109**

Abstract

Light reflected from Spectralon, the material chosen for on-board radiometric calibration of the Multi-angle Imaging SpectroRadiometer (MISR) is quantified in terms of the fraction of the reflected intensity that has the same polarization as the incident light. This fraction was measured for both s- and p-polarized incident light as a function of angles of incidence and reflection at three laser wavelengths of 442, 632.8 and 859.9 nm. At all wavelengths, the fraction is found to increase with both increasing angle of incidence and angle of reflection corresponding to a reduction in the depolarization of the incident beam, and the effect is greater for the incident perpendicular polarization state to the incident plane for forward scattering. Conversely, the incident parallel polarization state has a larger fraction at the large backward scattering angles. The percent polarization of the reflected radiation for an unpolarized source is obtained using these data. The percent polarization becomes negative at the large backward scattering angles indicating that the crossed polarized reflected component is larger than the parallel polarized reflected component. These observations are consistent with previous measurements of an enhanced off-specular peak in the Spectralon bidirectional reflectance function measured at large angles of incidence and reflection.

Measurement of the Depolarization of Reflected Light from Spectralon

D.A. Haner and B.T. McGuckin

Jet Propulsion Laboratory

California Institute of Technology

4800 Oak Grove Drive

Pasadena CA 91109

1. Introduction

The utilization of On-Board Calibrator (OBC) systems on satellite remote sensors has stimulated interest in materials for diffuse reflectance standards. For example, the Sea Viewing Wide Field Sensor (SeaWiFS) includes a diffuse panel made of a white thermal control paint YB71 for the OBC during periodic viewing of the moon. Alternative materials for OBC's such as SpectraIon, a pure sintered polytetrafluoroethylene (PTFE) type material supplied by Labsphere Inc., has been the favored choice for use on the Moderate Resolution Imaging Spectrometer Nadir/ Tilt (MODIS-N/T) and the Multi-angle Imaging SpectroRadiometer (MISR) instruments which belong to the suite of NASA Earth Observing System (EOS) sensors..

The MODIS instrument will be the first to use SpectraIon as an in-flight OBC and will provide one calibration path in conjunction with multiple OBC's, each using a different approach (Sun,

integrating sphere, spectroradiometer)¹. However, for MISR two Spectralon panels, together with their associated deploying mechanisms and calibration diodes constitute the entire OBC^{2,3} system. The diffuse panels will be deployed at approximately monthly intervals over the poles to reflect solar irradiance into each of the “pushbroom” camera banks for in-flight calibration and will otherwise be stowed and protected when not in use.

Therefore, in preparation for their deployment on MISR, a number of Spectralon panels have undergone an extensive series of pre-flight tests of the optical reflectance characteristics. It is the objective of this paper to report on these tests with emphasis on quantifying the depolarization of incident light upon reflection from Spectralon. Knowledge of the depolarization of light is especially important for modeling of the panel response for those occasions during the on board calibration process when the sunlight which is incident on the panel has traversed the Earth’s limb and has become partially polarized in consequence of the atmospheric scattering processes. In the case where the incident light is not polarized there is partial polarization of the reflected light from the calibration plates, and this must be considered if any of the on board detectors have polarization sensitivity.

The data will be presented graphically as the fractional polarization component with the angle of reflection as the abscissa, The fractional polarization component is defined as the fraction of the reflected intensity that has the same polarization as the incident light. The data will be combined on an absolute basis to present “the fraction of polarization” of the reflected light for an unpolarized source.

2. Optical System

The optical setup of the directional reflectance characterization facility is a slightly modified version of that described earlier ⁴ and is illustrated in Figure 1. The three wavelengths chosen are all derived from laser sources, which are a helium cadmium (HeCd) lasing at 442 nm, a helium neon (HeNe) laser at 632.8 nm and a GaAlAs semiconductor diode laser source at 859.9 nm. A second half-waveplate (zero-order) at each wavelength is used to set the polarization of the incident beam to either p- or s-polarized relative to the principal plane which contains the Spectralon normal, the incident wavevector and the detector axis. A 500:1 extinction ratio polarizer cube is mounted in a calibrated rotation stage and located immediately in front of the detector telescope assembly which is used to view the light scattered from the panel. The polarizer aperture is sufficiently large to avoid compromising the 20 angular resolution of the telescope. Polarizer rotation by 90° at the detector between angular data runs permits resolution of the scattered light into its orthogonal components, each of which is measured separately. The Spectralon test piece examined is 7.5 x 5.0 x 0.6 cm in size and cut from the same piece of material as the proto flight panels previously studied ⁵. Experiments have established the correlation between the reflectance response of the test piece and the proto flight panels to be - 0.4%, which included each polarization incident over large ranges of experimental conditions. This small variation gives confidence that the test piece depolarization characteristics can be transferred to the protoflight panels. To describe the plane of polarization measurement at the detector with reference to the incident plane of polarization two letters are used, the second letter denotes the polarization preference at the detector. Thus sp indicates the incident

polarization is s and the detector views p.

In order to make comparison of polarization data possible on a quantitative basis the reflectance detector voltage is calibrated to the incident irradiance for all data at a given wavelength using calibrated neutral density filters. The measurements were duplicated at each of the other wavelengths where each data point corresponds to an average of 1000 samples recorded at 10 ms intervals, and the measurement precision and system repeatability between runs is at the 0.2% level. For each polarization state incident on the test piece, and with beam angles of incidence of 0°, 30°, 45° and 60°, the bidirectional reflectance function (BRF) is measured with the analyzer positioned to pass s- and then p- polarized light onto the silicon photo diode, which is rotated through the range of $-85^\circ < \theta_r < 85^\circ$ with 50 increments where negative sense denotes the direction of backward scattering referenced to the surface normal. In each case, the fractional polarization component, DR_{xx} , is calculated for each value of θ_r using:

$$DR_{pp} = \frac{I_{pp}}{(I_{pp} + I_{ps})} \quad \text{or} \quad DR_{ss} = \frac{I_{ss}}{(I_{sp} + I_{ss})}$$

where the intensity $I_{pp,ss}$ is the calibrated detector response for the component parallel to the incident polarization, and the denominator is the sum of the calibrated polarization resolved components. If there were no depolarization upon reflection DR_{xx} would be unity; and if the incident radiation were completely depolarized upon reflection DR_{xx} would be 0.5. The complement of the fractional polarization component can be found by noting for example, $DR_{sp} = 1 - DR_{ss}$. Further the fraction of polarization for a polarized source is defined as:

$$P_s = DR_{ss} - DR_{sp} = \frac{I_{ss} - I_{sp}}{I_{ss} + I_{sp}} = 2DR_{ss} - 1$$

and the s depolarization is: $I_{sp}/I_{ss} = (1 - DR_{ss})/DR_{ss}$.

Combining all polarization data at a single angle of incidence provides an estimate of the fraction of polarization for an unpolarized source at each angle of incidence:

$$P_\theta = \frac{(I_{ps} + I_{ss}) - (I_{sp} + I_{pp})}{I_{ps} + I_{ss} + I_{pp} + I_{sp}}$$

The presentation of the data will be limited to the fractional polarization component for each incident polarization state as DR_{ss} , DR_{pp} , and the fraction of polarization for an unpolarized source, P_θ , as a function of the angle of reflection for 0° , 30° , 45° and 60° angles of incidence for wavelengths: 859.9 nm, 632.8 nm, 442 nm.

3. Results and Discussion

The reflectance depolarization properties of Spectralon at 859.9, 632.8, and 442 nm are in general very similar. These general features will be discussed in detail and the complete spectrum of measurements at 859.9 nm are included and are shown in Figs. 2 and 3.

The first reflectance feature to be recorded is that there is no discernible specular reflection from the surface under any experimental conditions.

The fractional polarization component (DR_{xx}) is shown in the composite Fig. 2, where the figure composites a, b, c, and d correspond to the beam incidence of 0° , 30° , 45° and 60° with the abscissa being the angle of reflectance.

Fig. 2 shows the fractional polarization component for the two incident polarizations and prompts the following comments:

When the angle of incidence is zero degrees (Fig. 2a, normal incidence) the definition of s and p are not distinct and the fractional polarization component for the experimental set-up for initialization give the same value for all view angles which is also constant to within 0.025 of the value 0.516. This value corresponds to a depolarization of 0.938 which is within 6% of perfect depolarization of the incident radiation. The retro reflection peak is not visible as it is in the shadow of the detector which also causes the large discontinuities in the graphical presentation at the angle of incidence. While all the data used to compose the figures were carefully energy calibrated the fractional polarization component curves of s and p incident polarization do not coincide as would be expected for a homogeneous scattering material. These differences are on the 2% level and indicate the level of operational experimental precision.

At an angle of 30° , Fig. 2b, the fractional polarization component for s incidence is seen to increase monotonically from the back scattering angles to the maximum forward angle. This distribution would correspond to scattering from a surface composed of randomly oriented facets where the s polarization would dominate in the forward direction since it should be more efficiently reflected'.

A fraction of the irradiance is transmitted into the surface to be multiply scattered isotropically with increased depolarization. In contrast, the fractional polarization component for the p incidence is seen to be a curve with curvature reaching a minimum at 20° angle of reflection. The curve in the forward direction indicates that the material depolarizes the reflected radiation more than in the case of s incidence. This can be explained by recalling that classically the p polarization incident on a surface is preferentially transmitted into the material. This suggests that the p polarized irradiance will contribute most efficiently to the multiple scattering, which is depolarizing and is radiated more uniformly in all directions.

At an angle of incidence of 45° , Fig. 2c, the general features of the fractional polarization component remain unchanged, but the maximum value in the forward direction has increased by about 14% for the s incident and by about 8.5% for the p incident. This general increase of fractional polarization component in the forward directions with increased angle of incidence is shown in Fig 2d. At a 60° angle of incidence, the s incidence increases by 25% and the p incidence increases by 2.5%. Whereas the difference in the fractional polarization component in the s and p incidence at the large backward angles has increased only slightly. These features are generally duplicated at 632 and 442 nm.

Fig. 2b, 2c, and 2d shows that the fractional polarization component for the s and p radiances have the same value at about -200° and that the fractional polarization component for p incident is larger and is increasing for larger negative angles which corresponds to decreasing depolarization. This corresponds to the back scattered light having a smaller fraction of s component relative to p

component, This feature of the fractional polarization component is also present for 450 and 60° angles of incidence.

Fig. 2b, 2c, and 2d show that the fractional polarization component has increased for the large forward scattering angles as the angle of incidence has increased. This trend is expected for s polarized irradiance reflected from a well defined surface. The difference between the s and p fractional polarization component increases in the forward direction due mostly to the increase in the s component even though there is an increase in the p component in the forward direction.

The most significant feature in the depolarization data is that the p fractional polarization component is larger than the s fractional polarization component for backward angles. This behavior is called negative polarization and is a recognized property of materials characterized as volume scatterers. For the spectralon at 859, 632, and 442 nm, the inversion angle (the angle where the curves intersect) is consistently between -200 and 150. The angle of inversion is not precisely defined due to the fact that both depolarization curves have nearly the same slope and value in the neighborhood of the crossing. An average of -6° would be indicated due to the relative variations in the data sets. The variation present in the data is probably due to experimental error or is an indicator of the calibration error between the data sets

The primary interest in the polarization experiment was to collect data that would describe the reflection polarization from the material by an unpolarized source such as the sun. In order to obtain some estimate of the fractional polarization from an unpolarized source reflecting from this material

all the polarization data are combined after energy calibration. The fraction of polarization, PO , is shown in composite Fig. 3 for 859.9 nm. The figure composites a, b, c, and d correspond to the beam incidence angles of 0° , 30° , 45° and 60° versus the angle of reflectance.

For the 0° incidence irradiance, the s and p polarization planes are not uniquely defined and the fraction of polarization would be expected to be zero which is the case to within about 1%. The fraction of polarization at the large angle of reflection shows large variations due to the fact that the results are from the subtraction of small numbers, thus emphasizing the experimental noise. As the incidence angle of the irradiance increases, the fraction of polarization curves develop a slope with increasing curvature in the forward scattering direction. The inversion angle occurs at the reflectance angle of about -20° where the fractional polarization component for s and p were equal. The fraction of polarization at the greatest backward scattering angle is nearly constant at all angles of incidence; however it is an increasing function of incidence angle in the forward direction.

A summary of the depolarization results of reflected light from Spectralon is presented in Table 1. The topics presented in the table are fractional polarization component, fraction of polarization for large backward and forward scattering angles, and the inversion angle; grouped by the angle of incidence for the three wavelengths: 859, 632, and 442 nm. Examination of the values in the table leads to the following observations. It is evident that the depolarization is less at large view angles and the difference between the scattered s- and p- components diverges with increasing θ_r . This behavior is consistent with specular reflection from a surface composed of randomly oriented mirror-like facets^{6,7}. Reflectance from Spectralon is a combination of a diffuse component due to internal scattering and an off-specular component due to reflection from the surface facets. The

effect of the latter are more evident at large angles of incidence and reflections. The reduced depolarization with increasing view angle (**in which** the DR_{xx} departs from an ideal value of 0.5, corresponding to perfect depolarization by the panel) is a consequence of the enhanced surface contribution to the total panel reflectance observed under these conditions-- especially visible at $\theta_i = 60^\circ$. Evidence for the surface effect was obtained previously and is manifest by the presence of an off-specular peak in the BRDF plots⁵. The observation that the s- component reflectance is always greater than that of the p- component is corroborative evidence in support of the proposed reflection mechanism from Spectralon.

This surface characteristic was attributed to the relative scale of the surface roughness resulting from the manufacturing process. However the polarized measurements do not show that this surface feature changes with wavelength. The fractional polarization component graphs for wavelengths 632.8 and 442 nm are similar to the data presented in Figs 2 and 3 and are nearly identical in shape.

Conclusions:

The depolarization of light from a Spectralon test piece which is representative of the MISR flight panels has been measured for both s- and p-polarized incident light as a function of angle of incidence and reflection at three laser wavelengths. At all wavelengths, for $\theta_i = 0^\circ, 30^\circ, 45^\circ$ and 60° and over the range of reflectance angles $-85^\circ < \theta_r < 85^\circ$, the fractional polarization component, DR_{xx} , is consistently observed to increase with θ_i . These data will enable those who choose Spectralon for the calibration of flight instruments to accurately model the instrument response when polarized light is incident on the panels or if the detectors are polarization sensitive and the incident light is unpolarized. The results of these measurements are qualitatively consistent with the results

of earlier researchers^{8,10}.

While an estimator of the fraction of polarization of the reflected light for an unpolarized source has been presented here, it must be remembered that the sources in these experiments were polarized lasers. The question remains unanswered as to whether there may be any causes of significant differences in the measured fraction of polarization for narrow band incoherent irradiance.

Acknowledgments:

This work was carried out at the Jet Propulsion laboratory, California Institute of Technology, under contract with the National Aeronautics and Space Administration (NASA). D.A. Haner is a member of the Chemistry Department, California State Polytechnic University, Pomona CA. The authors acknowledge the technical support of S. Dermenjian, C. Esproles and A. Brothers and also valuable discussions with R.T. Menzies, C.J. Bruegge and V. Duval.

References

- (1) Bruce Guenther, V. Salomonson, W. Barnes, E. Knight, J. Barker, J. Harnden, G. Godden, H. Montgomery, and P. Abel, "MODIS Calibration: A brief review of the strategy for the at-launch calibration approach," *J. of Atmos. and Oceanic Technol.*, **13,274-285** (1996)

- (2) C.J. Bruegge, A. E. Steigman, R. A. Rainen and A. W. Springstein “Use of SpectraIon as a Diffuse Reflectance Standard for In-Flight Calibration of Earth Orbiting Sensors,” *Opt. Eng.* 32, 805-814 (1993)
- (3) C. J. Bruegge, V. G. Duval, N. L. Chrien and D. J. Diner, “Calibration Plans for the Multi-angle Imaging SpectroRadiometer (MISR),” *Metrologia*, 30, 213-221 (1 993)
- (4) B. T. McGuckin, D. A. Haner, R. T. Menzies, C. Esproles and A. M. Brothers,” “Directional Reflectance Characterization Facility and Measurement Methodology,” *Appl. Opt.* 35,4827-4834 (1996).
- (5) B. T. McGuckin, D. A. Haner, and R. T. Menzies, “Multi-angle Imaging SpectroRadiometer (MISR): Optical Characterization of the On-Board Calibration Panels,” To be published in *Applied Optics*
- (6) K. E. Torrance and E. M. Sparrow, “Polarization, Directional Distribution and Off-Specular Phenomena in Light Reflected from Roughened Surfaces” *J. Opt. Soc. Am.*, 56, 916-925 (1966)
- (7) K. E. Torrance, “Theoretical Polarization of Off-Specular Reflection Peaks,” *J. Heat Transfer*, 91, 287-290 (1969)

- (8) D.C. Cramer and M. E. Bair, "Some Polarization Characteristics of Magnesium Oxide and Other Diffuse Reflectors," *Appl. Opt.* 8, 1597-1605 (1969)
- (9) G. C. McCoyd, "Polarization Properties of a Simple Dielectric Rough Surface Model," *J. Opt. Soc. Am.* 57, 1345-1350 (1967)
- (10) W. G. Egan, J. Grusauskas, and H. B. Hallock, "Optical Depolarization Properties of Surfaces Illuminated by Coherent Light," *Appl. Opt.* 7, 1529-1534 (1968)

FIGURE CAPTIONS

Figure 1. Detail of the Spectralon test piece orientation relative to the incident beam and the detector position.

Figure 2. Fractional polarization component for a coherent source at 859.9 nm. Composites are for angles of incidence, 0° , 30° , 45° and 60° as indicated, reflected from Spectralon.

Figure 3. Fraction polarization for a coherent source at 859.9 nm. Composites are for angles of incidence, 0° , 30° , 45° and 60° as indicated, reflected from Spectralon.

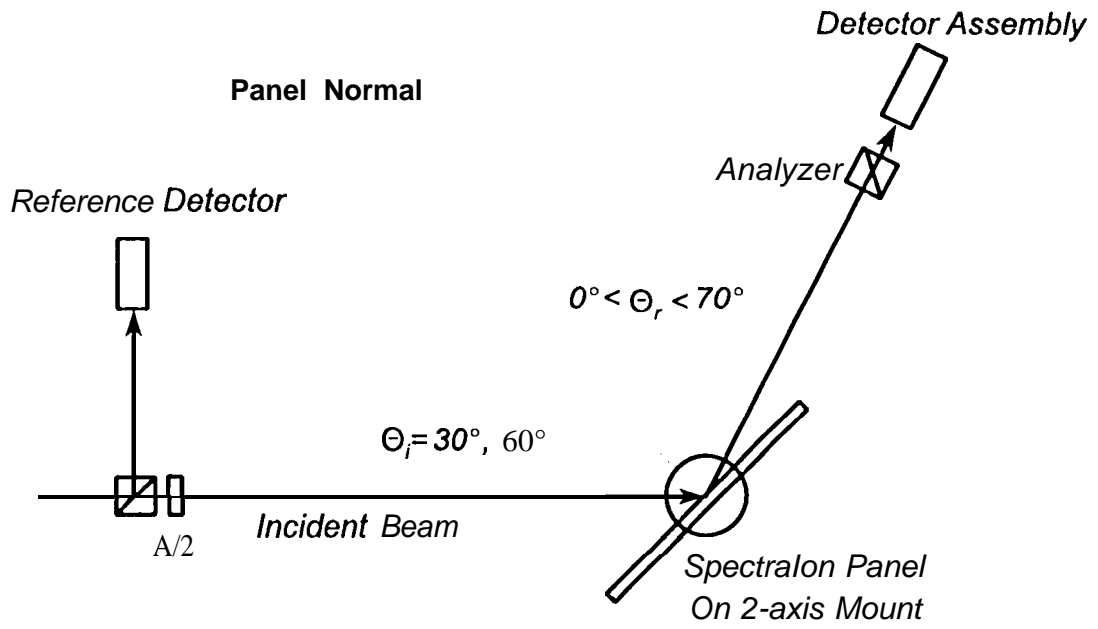
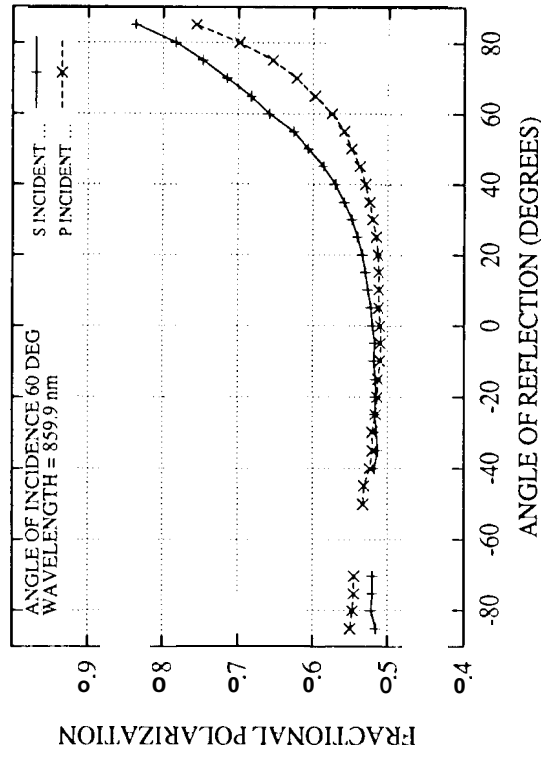
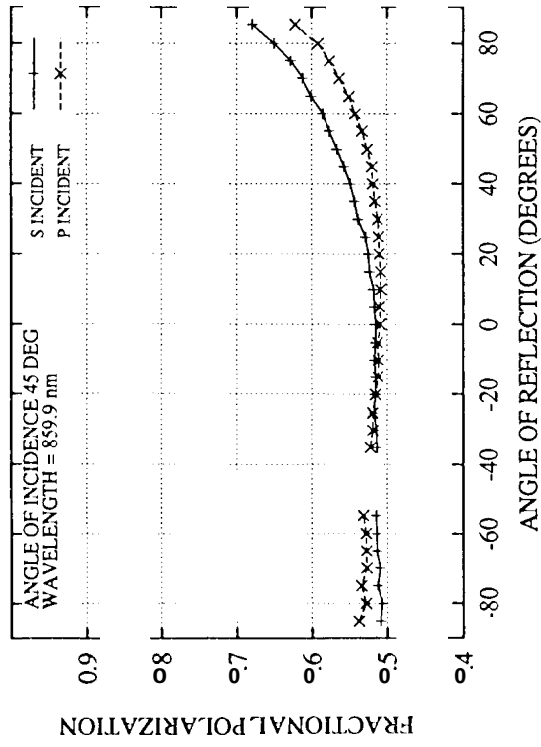
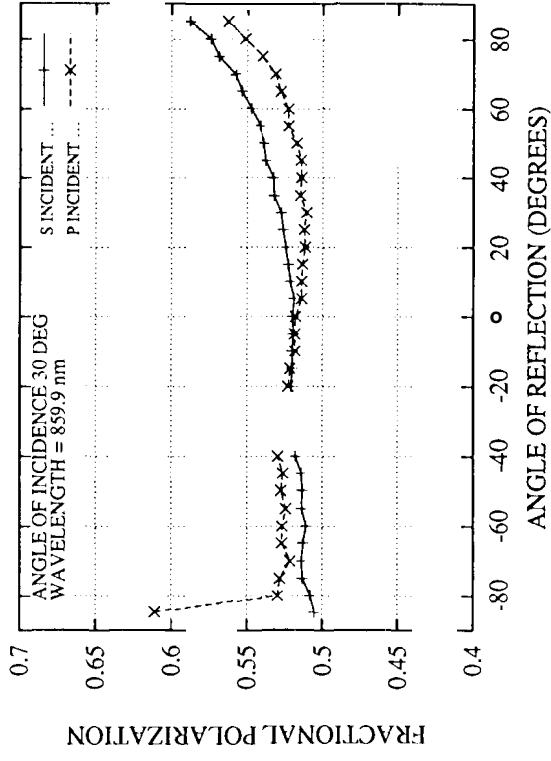
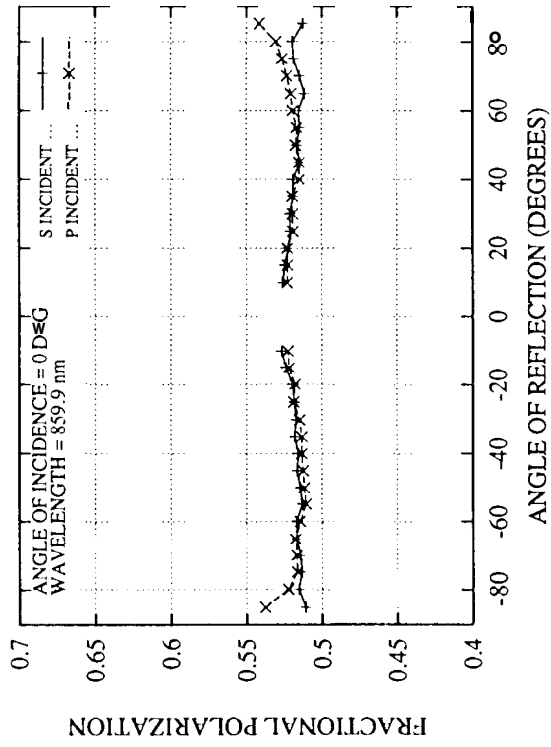
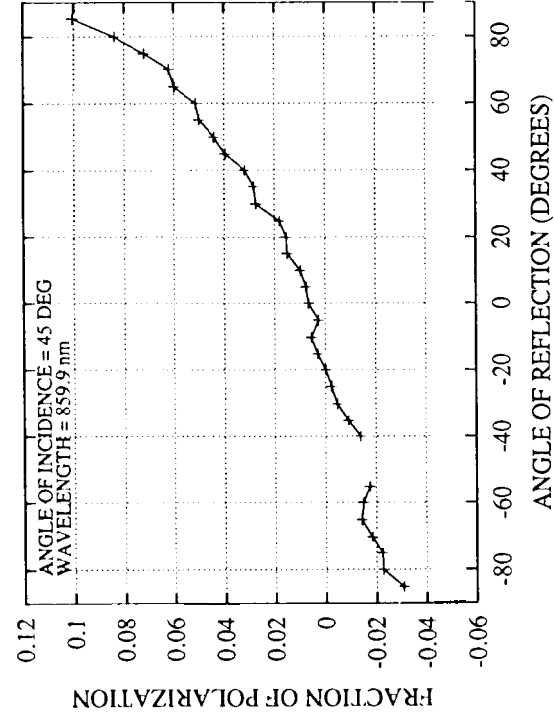
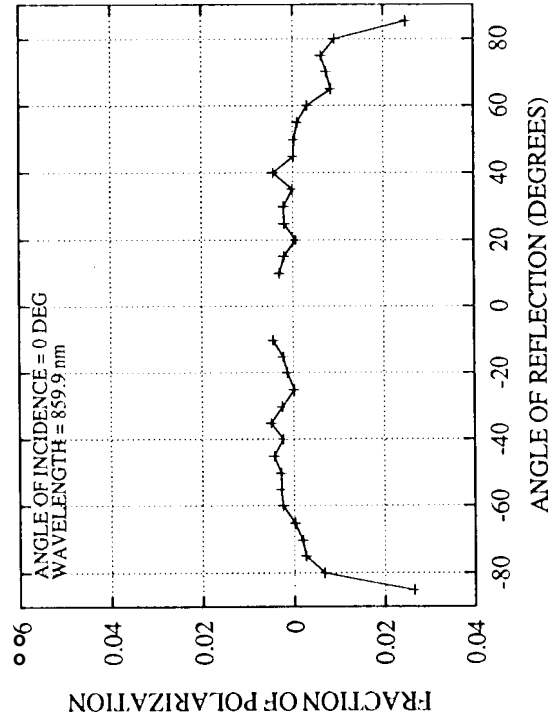
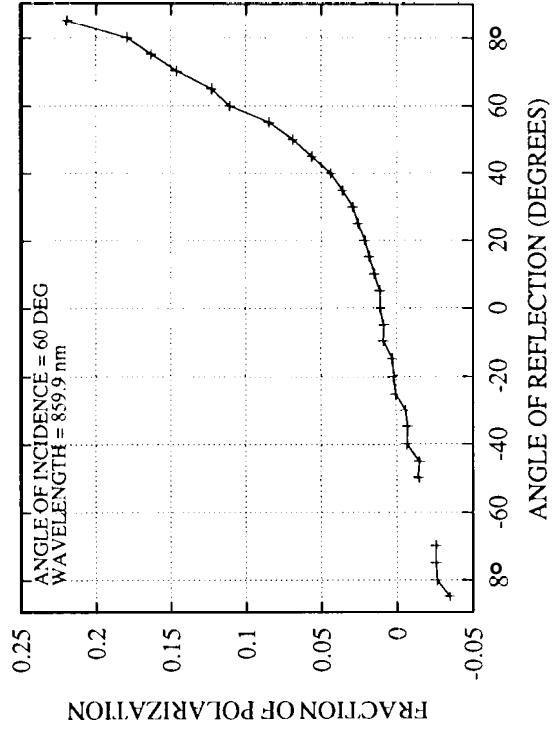
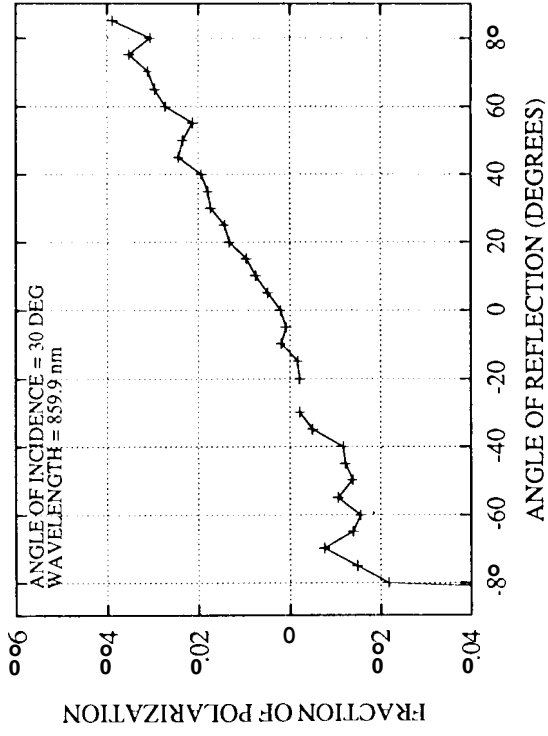


Figure 1.





	Fractional Polarization				Fraction of Polarization		Inversion Angle	
	θ_i	$\theta_r = -80$		$\theta_r = +80$		$\theta_r = -80$	$\theta_r = +80$	θ_r
		S	P	S	P	I		
859.9 nm	30	0.51	0.53	0.58	0.55	-0.020	0.034	-20
	45	0.51	0.53	0.65	0.59	-0.023	0.084	-20
	60	0.52	0.55	0.78	0.70	-0.026	0.180	-20
632.0 nm	30	0.50	0.53	0.57	0.56	-0.026	0.030	+18
	45	0.50	0.53	0.57	0.56	-0.026	0.033	+18
	60	0.51	0.55	0.78	0.69	-0.038	0.180	+5
442.0 nm	30	0.50	0.52	0.57	0.54	-0.017	0.039	-20
	45	0.50	0.52	0.64	0.58	-0.027	0.084	+5
	60	0.51	0.54	0.77	0.67	-0.025	0.180	-25